High-index sensitivity of surface mode in photonic crystal hetero-slab-edge microcavity

Tsan-Wen Lu,* Yi-Hua Hsiao, Wei-De Ho, and Po-Tsung Lee

Department of Photonics and Institute of Electro-Optical Engineering, National Chiao Tung University, Rm. 415 CPT Building, 1001 Ta-Hsueh Road, Hsinchu 300, Taiwan

**Corresponding author: ricky.eo94g@nctu.edu.tw*

Received January 15, 2010; revised March 24, 2010; accepted March 25, 2010; posted April 1, 2010 (Doc. ID 122763); published April 30, 2010

We introduce a photonic crystal hetero-slab-edge microcavity design with surface mode, which is beneficial for optical index sensing. The simulated index sensitivity (R_n) as high as 675 nm per refractive index unit (nm/RIU) variation is obtained with slab thickness of 180 nm. In experiments, single surface mode lasing action from a real device is observed. Based on the surface mode in this microcavity, high experimental R_n value of 625 nm/RIU is achieved by detecting index variation in a CO_2 chamber with different gas pressures.

OCIS codes: 140.5960, 230.5298, 230.5750.

Optical index sensing via resonances in different photonic structures [1,2] has long been a practical tool in various research fields. Especially in biological researches, this approach provides a fast and precise way to detect very small variation of analytes. In recent years, various resonance structures have been reported for highly sensitive optical index sensors, including surface plasmon resonance [3], long-period grating fiber [4], silica ring and sphere resonators [5–7], etc., where the resonance wavelength shift is usually used to estimate the analyte variation. However, considering their device sizes, most of them may not be compact enough when we want to realize a versatile optical sensing integrated chip with very compact size. Fortunately, a photonic crystal (PhC), an artificial material with periodic dielectric variation, hosts the advantage of well-controlling photon flow in wavelength scale owing to the photonic band gap (PBG) effect. Various PhC micro- and nanocavities have been proposed (see [8–13] for the most recent works) to serve as optical sensors with advantages of high sensitivity and very compact size. The ultrasmall mode volume in PhC cavities also permits optical sensing with very low analyte consumption (typically, less than 1 fL) [9,12], which is beneficial for certain analyte with very limited amount.

In our previous work [14], we have proposed and demonstrated a PhC hetero-slab-edge (HSE) microcavity laser. In this design, the defect mode is confined in surface wave form at the PhC slab edge owing to PBG and total internal reflection effects. Compared with most defect modes confined inside PhC micro- and nanocavities [8–11], the surface mode energy field extends more into the environment, which is very beneficial for optical index sensing because of the strong interaction between surface mode and environmental analytes. Based on this PhC HSE microcavity design, in this Letter, we reduce the microcavity slab thickness to obtain high index sensitivity (R_n, defined as wavelength shift per refractive index unit variation, nm/RIU) for serving as an optical index sensor. In experiments, we demonstrate the surface mode lasing in a PhC HSE microcavity and its highly sensitive optical index sensing functionality by detecting CO_2 with different pressures.

In a 2D truncated PhC slab, shown in Fig. 1(a), the surface wave will form and propagate along the interface between the dielectric PhC slab and air, as shown by the simulated electric field distribution in the inset of Fig. 1(a). Different truncated PhC slab

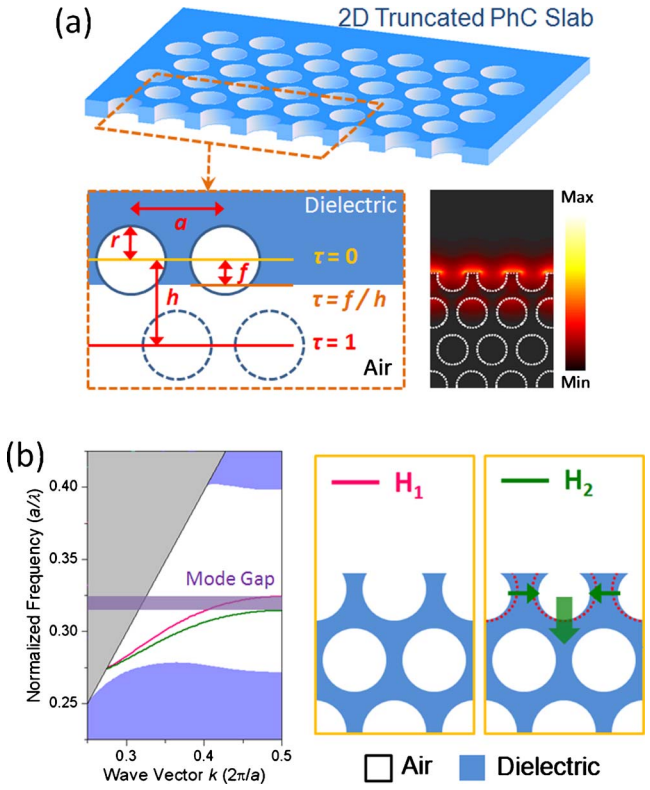

Fig. 1. (Color online) (a) Scheme of 2D truncated PhC slab surrounded by air and the definition of slab-edge termination parameter τ. The simulated surface mode in electric field propagating along the slab edge with τ=0.25 is also shown in the inset. (b) Calculated dispersion curves of surface modes propagating along the PhC slab edges H_1 and H_2. The dark gray (purple online) shadow represents the mode gap formed by H_1 and H_2.

terminations with τ defined in Fig. 1(a) will lead to different surface wave properties [15]. For two different slab edges, H_1 and H_2, shown in Fig. [1(b)], where the H_2 slab edge is obtained by shrinking and shifting the air holes at the slab edge of H_1, the allowed surface mode frequency in H_2 will shift to be lower than that in H_1, as shown in the band diagram of Fig. [1(b)]. The mode gap, denoted by a shadow region in Fig. [1(b)], will form owing to the surface mode frequency difference between H_1 and H_2; that is, the surface mode in H_1 with frequency inside the mode gap cannot propagate in H_2. Thus, the hetero-interface H_1/H_2 can serve as a mirror.

By applying double hetero-interfaces mentioned above, we can obtain a PhC HSE microcavity with high quality (Q) factor surface mode, as shown by the scanning electron microscope picture in Fig. 2. The surface mode in microcavity region with slab edge H_1 will be confined by mode gap effect provided by the gradually varying and outer barriers with slab edges H_G and H_2. For gradually varying barrier H_G, the radii and positions of air holes at the slab edge are shrunk and shifted gradually and linearly. The air-hole radius (r) over lattice constant (a) (r/a) ratios of the remaining outer barrier H_2 are kept invariant, and the r/a ratio difference between H_1 and H_2 is denoted as $\Delta r/a$. In 3D finite-difference time-domain (FDTD) simulations, we optimize the Q factor by tuning $\Delta r/a$ and the length of H_G at fixed τ. High Q value of 6.6×10^5 is obtained when the gradually varying barrier length of H_G, cavity length with H_1, slab thickness, $\Delta r/a$, and τ are $5a$, $10a$, 220 nm, 0.04, and 0.25, respectively.

To obtain high R_n value of the confined surface mode, in simulations, the slab thickness is reduced from 220 nm to be 150 nm, which is thinner than typical half-wavelength design ($\lambda/2n$, ~220 nm for $\lambda=1500$ nm and $n=3.4$). This leads to more extension of mode field outside the cavity and increases the interactions between light and environmental index variation. In Table 1, the simulated R_n value increases from 625 to 720 nm/RIU with the slab thickness reduced from 220 to 150 nm, where R_n value is estimated by the resonance wavelength shift under

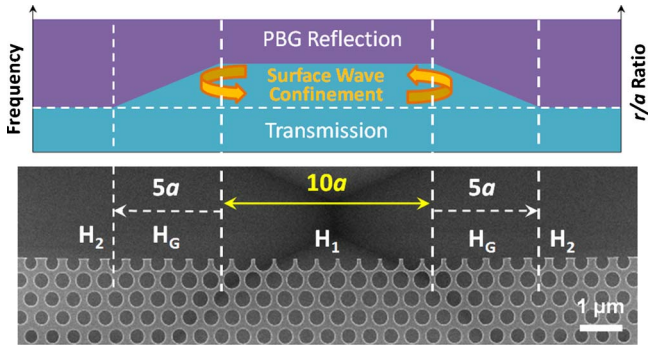

Fig. 2. (Color online) Scheme of PhC HSE microcavity with cavity (H_1), gradually varying barrier (H_G), and outer barrier (H_2) layers. The r/a ratio distribution and the formed mode gap in frequency by these three regions are also illustrated. The r/a ratio of H_1 and a of the fabricated microcavity are 0.38 and 540 nm, respectively.

Table 1. FDTD Simulated R_n, Mode Volume, and Q Factor of PhC HSE Microcavities with Different Slab Thicknesses

Slab Thickness	R_n	Mode Volume	Q
220 nm	625 nm/RIU	2.25 $(\lambda/n)^3$	6.6×10^5
180 nm	675 nm/RIU	2.14 $(\lambda/n)^3$	3.2×10^5
150 nm	720 nm/RIU	2.03 $(\lambda/n)^3$	1.1×10^5

0.02 index variation in simulations. In addition, the surface mode volume also decreases with the reduced slab thickness. Owing to its small mode volume, as an optical index sensor, the analyte consumption would be about 2 fL. In the following experiments, the slab thickness is chosen as 180 nm according to our currently available epitaxial structure.

The PhC patterns are defined by electron-beam lithography and followed by a series of dry- and wet-etching processes based on the epitaxial structure consisting of four compressively strained InGaAsP multi-quantum-wells with total thickness of 180 nm. The fabricated PhC HSE microcavity is optically pumped by a diode laser with pump spot diameter, pulse width, and duty cycle of 3.5 μm, 40 ns, and 0.2%, respectively, to avoid thermal problems. The measured lasing spectrum, polarization, and the light-in–light-out (L-L) curve of surface mode are shown in Figs. 3(a) and 3(b). The lasing wavelength, threshold, and polarized degree are estimated as 1572.5 nm, 0.9 mW, and 0.81, respectively.

To demonstrate optical index sensing functionality by a PhC HSE microcavity, we set up a high vacuum chamber with a gas flow controlling gauge and a vacuum pump. The device is mounted on a stage inside the chamber and can be observed from a quartz optical window by microphotoluminescence system outside. In preparation, the chamber is vacuumed down to the pressure of 10^{-2} Pascal (Pa) and then filled with CO_2 by the gauge. This procedure is repeated for three times to ensure that the chamber is filled with CO_2 only. CO_2 is an important analytic target in chemical analysis, biomedics, environmental monitoring, and so on. Besides, the use of CO_2 in our experiment provides very fine index variation

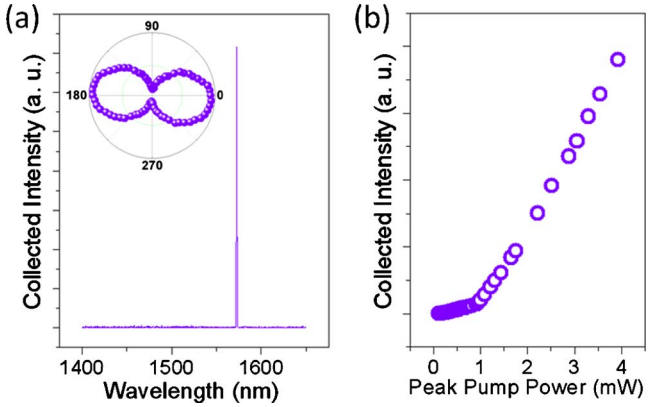

Fig. 3. (Color online) Typical (a) single-mode lasing spectrum, polarization, and (b) L-L curve of surface mode measured from PhC HSE microcavity laser.

and lower optical loss to the microcavity than in aqueous or organic solvent.

In the experiment, first, a PhC HSE microcavity is pumped for 30 min to guarantee the stability of the microcavity laser, which can be observed from the invariant lasing wavelength. The pump power and pump position are strictly fixed during the measurements to avoid unwanted wavelength shift contributed by the temperature instability inside the microcavity. Then the CO_2 gas pressure (for reference, ~38.5 Pa in the atmosphere) in chamber is controlled and tuned from 1.00×10^4 to 1.15×10^5 Pa by the gas flow gauge and vacuum pump. The measured surface mode wavelength shift is shown in Fig. 4(a), which indicates a linear redshift when the CO_2 gas pressure increases, that is, when the environmental index increases. This agrees quite well with the FDTD simulation prediction also denoted in Fig. 4(a). The surface mode spectra under CO_2 pressures of 1.00×10^4 and 1.15×10^5 Pa are shown in Fig. 4(b). The wavelength shift is 0.3 nm, and the pressure variation leads to the refractive index change of 4.8×10^{-4}. Thus, we obtain a high R_n value of 625 nm/RIU in experiment, which agrees with the simulation result of 675 nm/RIU quite well. Considering the surface mode line width of 0.24 nm by Lorentzian fitting in Fig. 4(b), the experimental minimum detectable index variation δn_{exp} is about 4×10^{-4}. This value is similar to or better than those in [9–13]. Although presently δn_{exp} is not as small as the theoretical δn of 7.2×10^{-6} calculated from Table 1 because of the broadened line width arisen from carrier dynamics in active device, by using laser device as a sensor, we can discard highly efficient light input/output designs needed in most passive devices and obtain the optical signal easily. This simplifies the device design both in laboratory prototype and real applications. On the other hand, we perform thermal conduction analysis using a finite-element method to simulate the temperature fluctuation of the microcavity caused by the changed CO_2 thermal conductivity ρ_{CO2} under different gas pressures. The ρ_{CO2} variation is only 1.8×10^{-5} W/m.K when the gas pressure varies from 1.15×10^5 to 1.00×10^4 Pa, which corresponds to 0.15 K increase in temperature of the microcavity.

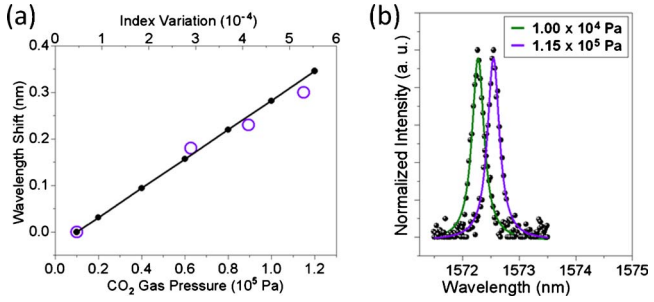

Fig. 4. (Color online) (a) Measured (open circles) and simulated (solid line with solid circles) wavelength shifts of surface mode under different CO_2 gas pressures and the corresponding index variations. (b) Surface mode lasing spectra under pressures of 1.00×10^4 and 1.15×10^5 Pa. The pump power is fixed at 1.5 mW.

This leads to the wavelength redshift smaller than 0.0075 nm in the InGaAsP-based microcavity [16], which is much smaller than above measured wavelength shift and can be ignored. Thus, we can conclude this wavelength shift is mainly contributed by the environmental index variation.

In summary, we have introduced and applied a PhC HSE microcavity with a highly index-sensitive surface mode for optical index sensing. To increase the R_n value of this microcavity, in 3D FDTD simulations, the slab thickness is reduced from typical half-wavelength design to be 150 nm, which leads to the increased R_n value from 625 to 720 nm/RIU. In experiments, single surface mode lasing action is observed from a PhC HSE microcavity with 180 nm slab thickness. Furthermore, we demonstrate the optical index sensing functionality by the surface mode wavelength shift under different CO_2 gas pressures in chamber. High experimental R_n value of 625 nm/RIU is achieved, which indicates the potential of the PhC HSE microcavity with the surface mode serving as a highly sensitive optical index sensor with a very compact size.

This work was supported by Taiwan's National Science Council (NSC) under contract numbers NSC-98-2120-M-009-002 and NSC-98-2221-E-009-015-MY2. The authors acknowledge the help from Center for Nano Science and Technology (CNST) of National Chiao Tung University, Taiwan.

References

1. C. Monat, P. Domachuk, and B. J. Eggleton, Nat. Photonics **1**, 106 (2007).
2. X. Fan, I. M. White, S. I. Shopova, H. Zhu, J. D. Suter, and Y. Sun, Anal. Chim. Acta **620**, 8 (2008).
3. J. Homola, S. S. Yee, and G. Gauglitz, Sens. Actuators B **54**, 3 (1999).
4. L. Rindorf, J. B. Jensen, M. Dufva, L. H. Pedersen, P. E. Høiby, and O. Bang, Opt. Express **14**, 8224 (2006).
5. M. Sumetsky, R. S. Windeler, Y. Dulashko, and X. Fan, Opt. Express **15**, 14376 (2007).
6. A. M. Armani, R. P. Kulkarni, S. E. Fraser, R. C. Flagan, and K. J. Vahala, Science **317**, 783 (2007).
7. A. M. Armani and K. J. Vahala, Opt. Lett. **31**, 1896 (2006).
8. M. R. Lee and P. M. Fauchet, Opt. Express **15**, 4530 (2007).
9. S. Kita, K. Nozaki, and T. Baba, Opt. Express **16**, 8174 (2008).
10. D. F. Dorfner, T. Hürlimann, T. Zabel, L. H. Frandsen, G. Abstreiter, and J. J. Finley, Appl. Phys. Lett. **93**, 181103 (2008).
11. T. Sünner, T. Stichel, S. H. Kwon, T. W. Schlereth, S. Höfling, M. Kamp, and A. Forchel, Appl. Phys. Lett. **92**, 261112 (2008).
12. S. H. Kwon, T. Sünner, M. Kamp, and A. Forchel, Opt. Express **16**, 11709 (2008).
13. A. Di Falco, L. O'Faolain, and T. F. Krauss, Appl. Phys. Lett. **94**, 063503 (2009).
14. T. W. Lu, Y. H. Hsiao, W. D. Ho, and P. T. Lee, Appl. Phys. Lett. **94**, 141110 (2009).
15. J. K. Yang, S. H. Kim, G. H. Kim, H. G. Park, Y. H. Lee, and S. B. Kim, Appl. Phys. Lett. **84**, 3016 (2004).
16. P. T. Lee, J. R. Cao, S. J. Choi, Z. J. Wei, J. D. O'Brien, and P. D. Dapkus, Appl. Phys. Lett. **81**, 3311 (2002).